UC Irvine
UC Irvine Previously Published Works

Title
Optically dilute, absorbing, and turbid phantoms for fluorescence spectroscopy of homogeneous and inhomogeneous samples

Permalink
https://escholarship.org/uc/item/7760p17b

Journal
Applied Spectroscopy, 47(12)

ISSN
0003-7028

Authors
Durkin, AJ
Jaikumar, S
Richards-Kortum, R

Publication Date
1993-12-01

DOI
10.1366/0003702934066244

Copyright Information
This work is made available under the terms of a Creative Commons Attribution License, availalbe at https://creativecommons.org/licenses/by/4.0/

Peer reviewed

eScholarship.org Powered by the California Digital Library
University of California

Optically Dilute, Absorbing, and Turbid Phantoms for Fluorescence Spectroscopy of Homogeneous and Inhomogeneous Samples

A. J. DURKIN, S. JAIKUMAR, and R. RICHARDS-KORTUM*
The Biomedical Engineering Program, The University of Texas at Austin, Austin, Texas 78712

This paper presents a phantom which simulates the optical properties of tissue. The phantom absorption coefficient, scattering coefficient, anisotropy factor, and fluorescence quantum yield can be independently varied to investigate the effects of these parameters on fluorescence excitation and emission spectra from 300 to 650 nm. Phantom fluorophores include Flavin Adenine Dinucleotide (FAD) and Rhodamine B. Absorption is controlled by adjusting phantom hemoglobin concentration. On the basis of their smoothly varying scattering coefficient and the relatively low amount of fluorescence contributed to the mixture in comparison to other available scatterers, 1.05-μm-diameter polystyrene microspheres were selected as a scatterer. Sample inhomogeneities are simulated by preparing the phantom in a gelatin substrate. The optical properties of turbid phantoms determined with the use of indirect techniques agree well with known values as long as $\mu_s(1 - g) > \mu_a$. Data are presented from dilute, absorbing, and turbid phantoms and inhomogeneous phantoms to qualitatively illustrate the effects of optical properties and sample geometry on fluorescence spectra. The phantom provides the framework for detailed quantitative investigations of the effects of optical properties, sample size, shape, and structure, boundary conditions, and collection geometry on fluorescence spectra.

Index Headings: **Fluorescence; Light scattering; Reflectance spectroscopy; Tissue simulation; Absorption; Tissue phantoms.**

INTRODUCTION

Although many biologically important molecules fluoresce, only limited attempts have been made to interpret tissue fluorescence spectra in terms of tissue chemical composition.[1,2] Instead, empirical algorithms have been employed to classify tissue type on the basis of fluorescence spectra, with impressive results.[3,4] Despite the success of empirical methods, a technique to relate tissue spectra to tissue chemistry is required to exploit the full potential of fluorescence diagnostics. Although extensive methodologies have been developed to analyze fluorescence spectra of dilute mixtures,[5,6] achieving such interpretation of tissue fluorescence is limited by several factors. Tissues consist of inhomogeneous mixtures of fluorophores with broadly overlapping excitation and emission spectra. These fluorophores are contained within an inhomogeneous scattering and absorbing matrix that affects the amount of excitation light which can reach the fluorophores and the amount of fluorescence which can escape the tissue surface and reach the detector.

Several analytic models have been proposed to relate fluorescence of homogeneous turbid media to the chemical composition of the sample.[1,7-9] Monte Carlo methods have been used to simulate tissue fluorescence spectra for a range of optical properties, boundary conditions, inhomogeneities, and excitation and collection geometries.[10-12] These studies have provided some insight into the information contained within the fluorescence spectra of turbid samples. However, no systematic experimental study has been undertaken to demonstrate the effects of changing optical properties, boundary conditions, degree of homogeneity, and collection geometries on the fluorescence spectra of turbid media.

This paper describes a phantom system with known optical and fluorescence properties which can be adjusted over the range exhibited by tissue in the UV/visible region of the spectrum. This phantom can be constructed as a homogeneous solution, or may be embedded in a gelatin matrix to model inhomogeneous samples.[13] By comparing fluorescence spectra of dilute, absorbing, and turbid solutions containing the same fluorophores, we derive an initial understanding of the effects of scattering and absorption on fluorescence. In addition, to investigate the effects of inhomogeneous sample composition on fluorescence spectra, we present fluorescence data from homogeneous and multilayer phantoms containing the same fluorophores. This phantom provides the basis for more extensive studies with a variety of boundary conditions, degrees of sample homogeneity, sample sizes, collection geometries, and optical properties.

IDEAL PHANTOM

An ideal phantom to simulate tissue fluorescence should provide the experimenter with independent control of the absorption coefficient, μ_a, the scattering coefficient, μ_s, the anisotropy factor, g, and the fluorescence quantum yield, ϕ. It is important to note that, while both fluorophores and absorbers contribute to the absorption coefficient, it is desirable that the scatterer be nonabsorbing and nonfluorescent. If this is achieved, the effects of absorption and scattering on fluorescence excitation and emission spectra can be studied systematically by directly comparing data from a dilute solution containing only fluorophores, a concentrated solution containing fluorophores and absorbers, and turbid samples containing either fluorophores and scatterers or fluorophores, absorbers, and scatterers. A final requirement of the ideal phantom is that the solution be stable, with no chemical interactions between various components or photobleaching during spectroscopic measurements. If these conditions are met, the absorption coefficient of the final mixture is simply the sum of the absorption coefficients of the individual constituents.

Received 4 June 1993.
* Author to whom correspondence should be sent.

0003-7028/93/4712-2114$2.00/0
© 1993 Society for Applied Spectroscopy

In general, optical properties vary with wavelength and tissue type. Ideally, the phantom should allow the experimenter to adjust the optical properties over the range demonstrated by human tissues. Absorbers and fluorophores within the phantom should exhibit absorption and emission peaks within the particular wavelength region of interest. In the UV and visible regions of the electromagnetic spectrum, tissue absorption coefficients vary from 0.2 to 25 cm^{-1}, while scattering coefficients vary from 25 to 400 cm^{-1}.[14] Tissue absorption coefficients are strongly wavelength dependent. Scattering coefficients are much less strongly wavelength dependent, decreasing with increasing wavelength in the range 250 to 700 nm. The anisotropy parameter of tissues, g, defined as the average cosine of the scattering angle, is typically nearly wavelength invariant, and is between 0.7 and 0.98 for most soft tissues.[14] Some typical values of optical properties for normal human aortic media at 560 nm are $\mu_a = 4.8\ cm^{-1}$, $\mu_s = 331\ cm^{-1}$, and $g = 0.89$, for a section 1100 μm thick.[10]

To develop a phantom for use in the 300–650 nm region of the spectrum, it is necessary to identify appropriate fluorophores, absorbers, and scatterers. The methods used to identify materials for inclusion in phantoms and to characterize their optical properties are described in the following section.

METHODS

Nonscattering Samples. Several measurements are required to characterize the optical properties of a phantom. In dilute solutions, which obey Beer's law, μ_a can be determined from transmission measurements as in Eq. 1 where T is the transmission, I_0 is the incident intensity, z is the sample thickness, and $I(z)$ is the transmitted intensity. The effects of mismatched boundary conditions can be removed by using double-beam instruments to measure transmission relative to that of an appropriate solvent blank.

$$T = \frac{I(z)}{I_0} = \exp^{-\mu_a z}. \quad (1)$$

To determine the total absorption coefficient of the nonscattering samples, we made collimated transmission measurements. These measurements were performed with a dual-beam absorption spectrophotometer (Hitachi U-3300). Transmission was measured from 250 to 700 nm in 0.5-nm increments. The resolution of the system was 2 nm, and scan time was 300 nm/min. The absorption coefficient was calculated at each wavelength with the use of Eq. 1.

Turbid Samples. Both direct and indirect methods have been proposed to measure optical properties of turbid samples.[15,16] Direct methods utilize collimated sources and thin samples to directly measure optical properties. Although direct methods require a minimum of computation, it is difficult to directly measure optical properties continuously as a function of wavelength, as is required for analysis of fluorescence data.[15] Indirect methods allow optical properties to be computed from measurements of total diffuse transmission and total diffuse reflection, which can be conveniently made over a wide wavelength range with a spectrophotometer equipped with an integrating sphere accessory.[16] Here, we use an indirect method to characterize the optical properties of the turbid phantoms.

Total reflection and transmission measurements were made for the scattering samples with the use of an absorption spectrophotometer (Hitachi U-3300) with a 90-mm-diameter Spectralon integrating sphere accessory. Experiments verified that, for scattering samples, significant amounts of light can escape through the sides of a 1-cm-pathlength cuvette.[17] These losses result in overestimation of the calculated absorption coefficient. Thus, samples were placed in 2-mm-pathlength quartz cuvettes in order to minimize the effects of light losses. The Fresnel reflection was collected for each scattering sample with the use of a 4° wedge accessory mounted at the rear port of the integrating sphere. The resolution of the system was 2 nm and the scan time was 300 nm/min.

When one is measuring diffuse reflection and transmission it is important to note that, unless this spectrophotometer is equipped with excitation and emission monochromators, fluorescence can contribute to the measured reflectance and transmission. At the fluorophore concentrations used in the phantoms presented here, measurements made with an instrument equipped with only an excitation monochromator (Hitachi U-3300) were equivalent to those made with an instrument with both excitation and emission monochromators (SPEX fluorolog II modified to measure reflectance). For samples containing nondilute concentrations of fluorophores [e.g., 300 μM Flavin Adenine Dinucleotide (FAD), 2-mm path; 4 μM Rhodamine B, 2-mm path], excitation and emission monochromators are required.[13]

Given the measured total diffuse transmission and reflection, the absorption coefficient and scattering coefficient can be determined iteratively.[16] In the iteration, one-dimensional diffusion theory with the delta Eddington phase function was used to calculate the reflection and transmission for a set of optical properties, these values were compared to the measured values of reflection and transmission, and the process was repeated until acceptable agreement was reached. Mismatched boundary conditions were incorporated in the calculation of total reflection and transmission. This method of determining optical properties requires that the anisotropy coefficient be known. The determination of the phase function of a sample in order to calculate the anisotropy factor can be difficult, particularly with highly forward scattering samples.[18] It is therefore particularly convenient that, for monodispersed particles with known uniform radius and index of refraction (as later adopted for use in our phantom), the anisotropy coefficient and the scattering coefficient can be calculated from Mie theory.[19]

Fluorescence. Fluorescence excitation-emission matrices (EEMs) were collected for all samples. Because variations in temperature can significantly affect the emission of fluorescence over the course of the acquisition of an EEM, refrigerated samples were allowed to equilibrate to room temperature[5] prior to data collection. Each sample was mounted in a 2-mm quartz cuvette. EEMs were collected at excitation wavelengths ranging sequentially from 320 to 490 nm in 5-nm increments with

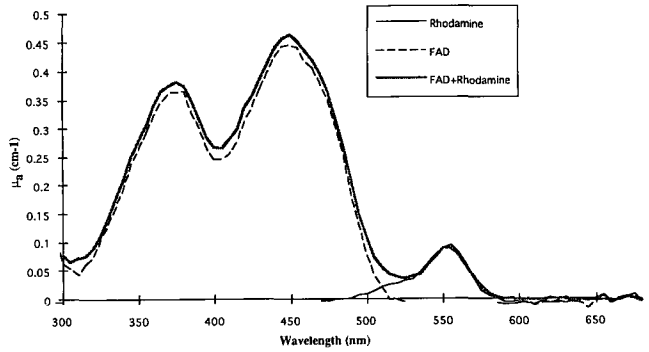

FIG. 1. Absorption spectra of dilute fluorophores. Concentrations of fluorophores were chosen in such a way that the sum of the optical densities at both the excitation and emission wavelengths was less than 0.1. This figure shows that the absorption coefficient of the mixture containing both 20 μM FAD and 0.43 μM Rhodamine B is the sum of the absorption coefficients of the individual fluorophores.

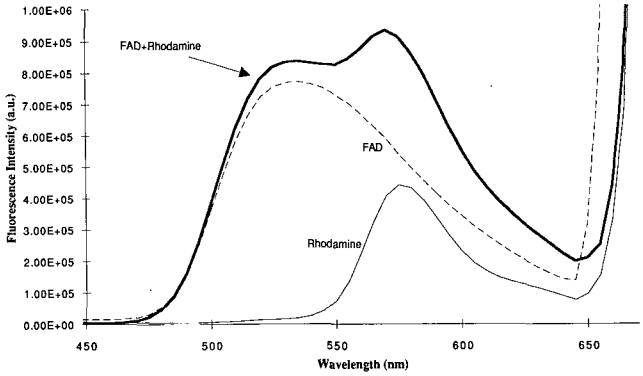

FIG. 2. Fluorescence emission spectra of 20 μM FAD, 0.43 μM Rhodamine B, and the mixture containing 20 μM FAD and 0.43 μM Rhodamine B. The excitation wavelength was 340 nm.

the use of a scanning spectrofluorimeter equipped with double excitation and emission monochromators (SPEX Fluorolog II). At each excitation wavelength, fluorescence emission was collected at 5-nm increments over a range starting at 10 nm longer than the excitation wavelength. Emission scans were terminated at a wavelength 10 nm less than twice the excitation wavelength or 700 nm, whichever was lower. The spectral resolution of the excitation and emission monochromators was 5.6 nm, full width at half-maximum (FWHM). The excitation beam was 2-mm × 2-mm square and was focused on the front face of the sample. The emission signal was integrated for 1 s at each excitation emission wavelength pair. Data presented here have been corrected for the nonuniform spectral response of the emission monochromator and photomultiplier tube with the use of correction factors supplied by the manufacturer. Variations in excitation intensity were corrected for with a Rhodamine B quantum counter.[20] The excitation intensity was always less than 40 μW/mm^2. Following collection of all emission spectra for a particular sample, the 340-nm excitation scan was repeated. Comparisons of the initial and final emission scans were used to assess the extent of any photobleaching. Fluorescence EEMs of solvent blanks were recorded and were subtracted from the spectra of nonscattering solutions to correct for solvent Raman scattering.

MATERIALS

All solutions were prepared in isotonic phosphate buffered saline (PBS, pH 7.4). Inhomogeneous samples were constructed from stacks of gelatin layers (4 g Knox unflavored gelatin and 120 mL PBS and chromophore) containing homogeneous distributions of fluorophores and chromophores. A thin sheet of plastic was used to separate layers to prevent chromophore diffusion between layers. Samples were placed in 2-mm-pathlength cuvettes for reflection, transmission, and fluorescence measurements.

Fluorophore Selection. Fluorophores with excitation and emission maxima in the region from 300 to 650 nm were identified from the literature.[5] Rhodamine B, with an absorption peak at 554 nm and an emission peak at 585 nm, and FAD, with absorption peaks at 370 nm and 450 nm and an emission peak at 515 nm, were chosen for their relatively high quantum yields. Rhodamine B was obtained from Exciton Laser Dyes Inc. and reagent-grade FAD was purchased from Eastman-Kodak. These were used without further purification. The fluorophore concentrations used in these phantoms are optically dilute.† Using published values of molar extinction coefficients for these chromophores,[21,22] we established that a 2-mm-pathlength solution was dilute for a mixture containing 0.43 μM Rhodamine B and 20 μM FAD. This was verified with the use of collimated transmission measurements for samples consisting of these fluorophores at these concentrations. The absorption spectra for these samples (Fig. 1) illustrate that, at dilute concentrations, the absorption coefficients of the individual fluorophores obey superposition when mixed together. Figure 2 shows that fluorescence sums linearly for dilute solutions of these chromophores. These fluorescence spectra were acquired at an excitation wavelength of 340 nm. Note that the same set of arbitrary units is used for fluorescence intensity throughout this paper. Solutions containing both FAD and NADH were also considered for use in phantoms. Experiments indicated that, although the fluorescence intensity of solutions containing only NADH was stable over many hours, the fluorescence of NADH in solution with FAD decreased by 30–50% over a period of 3 h. This decrease in fluorescence intensity indicates either quenching of NADH of fluorescence or oxidation of NADH to nonfluorescent NAD.[23] As a consequence, the combination of these fluorophores was removed from further consideration.

Absorber Selection. Absorbers with absorption maxima in the region between 300 and 650 nm and no fluorescence emission were desired. The literature indicated that oxyhemoglobin was likely to satisfy these requirements.[22,24] Oxyhemoglobin has absorption maxima at 420, 543, and 578 nm and is minimally fluorescent in this wavelength range.[22] These peaks fall in the fluorescence emission wavelength region of interest. The 543- and 578-nm absorption bands are located close to the 540-nm emission band of FAD and the 585-nm emission band of

† The sum of the optical densities at the excitation and the emission wavelengths is less than 0.1.[5]

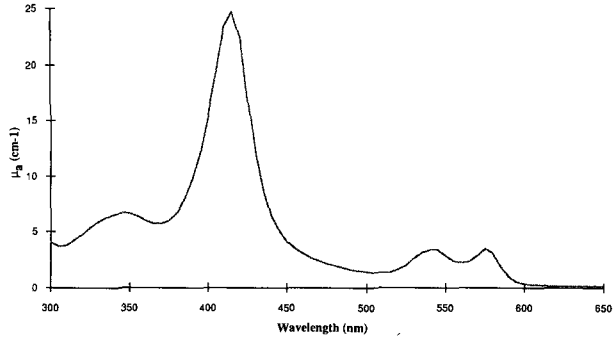

FIG. 3. Absorption spectra of hemoglobin obtained from human whole blood.

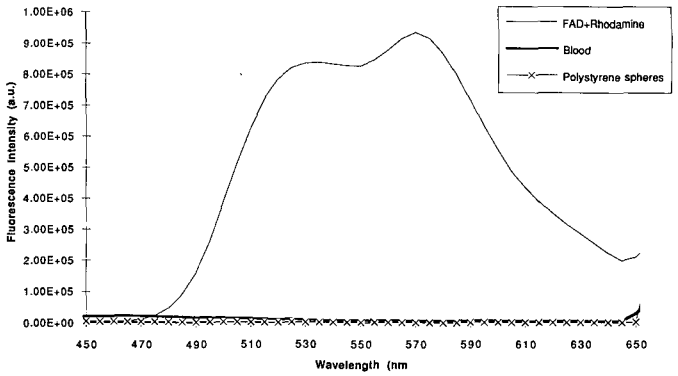

FIG. 4. Fluorescence emission spectra of hemoglobin and of 0.625% polystyrene spheres vs. fluorescence from a mixture containing 20 μM FAD and 0.435 μM Rhodamine B. The excitation wavelength of the incident light was 340 mm.

Rhodamine B. A typical absorption spectrum of oxyhemoglobin is shown in Fig. 3. Concentrations of absorber were investigated which provided total transmission greater than 1% at all wavelengths of interest in the phantom both with and without scatterer. Initial investigations were performed with the use of human hemoglobin purchased from Sigma Chemical Co. Because the purchased hemoglobin was relatively insoluble in PBS, fresh whole blood was selected as an alternative. Blood was drawn from one of us; hematocrit was determined to be 51%. Cells were lysed with the use of chilled, deionized water. Fragments of cell membranes were separated from the hemolyzed blood via centrifugation. The product was used as a source of oxyhemoglobin for the remainder of the study. The final concentration of hemoglobin used in each absorbing sample was the equivalent of 2% by volume red blood cells (RBCs). Collimated transmission measurements indicated that, as expected, the absorption coefficient scales linearly with concentration. Figure 4 illustrates the relative fluorescence intensities of hemoglobin and the dilute fluorescent solutions at concentrations used for this study. These emission spectra were collected for an excitation wavelength of 340-nm excitation. Hemoglobin fluorescence in this wavelength range is several orders of magnitude lower than FAD and Rhodamine B fluorescence.

Scatterer Selection. The ideal scatterer is nonfluorescent and nonabsorbing and yields diffuse reflectance and transmission similar to that of scattering tissues. Although a number of materials were investigated, a material exhibiting these properties that would stay in suspension throughout the course of an experiment could not be found. In reality, one must determine the level of fluorescence that results from each of the candidate scatters when used at concentrations necessary to give total diffuse reflection typical of tissue and select the material with minimum fluorescence. Intra-lipid (Lyposin II)[25] and glycogen[26] have been indicated for use in phantoms for reflection, transmission, or fluorescence depolarization studies of turbid samples. Other materials considered as scatterers for the phantom included milk, nondairy creamer, dextran, and polystyrene microspheres.

In order to identify which of these might be amenable to our investigations, the following experiments were undertaken: The concentration of scattering material in the phantom solution was increased until the total diffuse reflectance was in the range 10 to 35%—values typical for normal human aorta.[10] Glycogen and dextran were insoluble at the high concentrations required to simulate tissue scattering. Those samples that satisfied these reflectance and transmittance requirements were subjected to fluorescence measurements. The fluorescence of each scatterer was compared to that of dilute solutions containing the fluorophores of interest. Scatterers with fluorescence exceeding 10% that of the fluorophores of interest in the UV/Vis portion of the spectrum were excluded from further consideration. Table I gives the concentration of scatterer required to achieve the given diffuse reflectance and also lists the location (excitation, emission wavelength) and the value of the peak fluorescence intensity of the scatterer. Milk, nondairy creamer, and intralipid were dismissed from further consideration because each exhibits significant fluorescence in the wavelength region of interest here.

Although none of the scatterers investigated are nonfluorescent, polystyrene microspheres, purchased from Polysciences Inc., are an intermediate solution to this problem, with a fluorescence intensity of less than 1×10^4 counts (a.u.) at 340-nm excitation over the emission wavelength range from 350 to 650 nm at a concentration of 0.625% by volume. This fluorescence intensity is relatively insignificant compared to the peak fluorescence emission intensities at this same excitation wavelength for 0.43 μM Rhodamine B and 20 μM FAD (Fig. 4). It is important to note that we have observed that the fluorescence of polystyrene spheres can vary by more than a factor of two from lot to lot for a particular microsphere supplier. In addition to exhibiting minimal fluorescence, monodispersed polystyrene spheres enable one to use Mie theory to calculate the anisotropy coefficient and the scattering coefficient.[19] At these concen-

TABLE I. Materials that were investigated for use as scatterer in phantoms.

Scatterer	Diffuse reflectance	Maximum fluorescence (a.u.)	
		λ_{exc}, λ_{em} (nm)	Intensity
Lyposin II (0.25% by volume)	10–15%	(305, 417.5)	3.62×10^6
Milk (0.25% by volume)	10–20%	(355, 460.5)	2.46×10^6
Nondairy creamer (10 mg/L)	25–30%	(345, 412.5)	6.34×10^5
Polystyrene microspheres (0.625% by volume, 1.05-μm diameter)	20–35%	(305, 412.5)	3.60×10^5

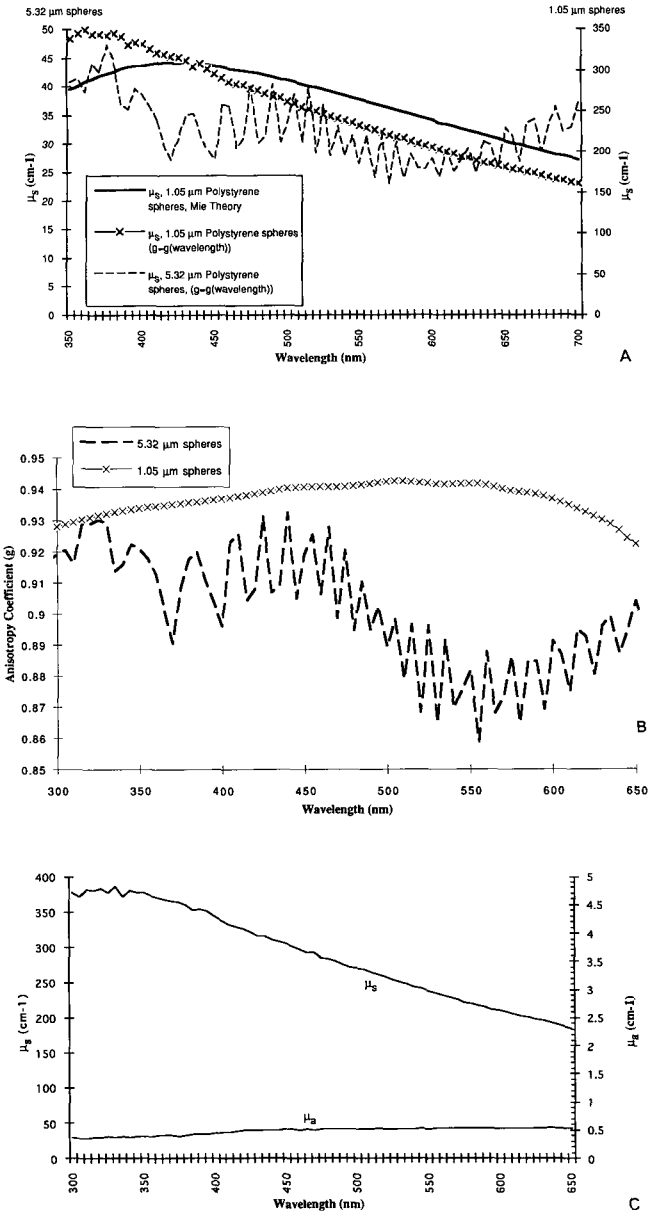

FIG. 5. (A) Experimentally determined scattering coefficients of 0.625% -by-volume 1.05-μm and 5.32-μm polystyrene microspheres and Mie theory prediction of 0.625% -by-volume 1.05-μm-diameter polystyrene microspheres. (B) Anisotropy coefficient calculated as a function of wavelength from Mie theory for 5.32-μm- and 1.05-μm-diameter polystyrene spheres. (C) The experimentally determined scattering and absorption coefficients of 0.625% polystyrene spheres.

trations, the polystyrene spheres remained in suspension for a period of several hours.

Having chosen a scattering material, one must select the size of sphere that most closely replicates the scattering phenomena typically seen in tissue. Two sizes of microspheres were examined in this study—1.05-μm diameter and 5.32-μm diameter. Diffuse reflection and transmission approaching those typical of tissue were obtained at concentrations of 0.625% -by-volume polystyrene spheres in PBS for both sizes of spheres. Optical properties were subsequently calculated from the reflectance and transmission data.

The experimentally determined scattering coefficients of a solution containing 0.625% -by-volume 1.05-μm- and 5.32-μm-diameter polystyrene microspheres are shown in Fig. 5A. In calculating μ_s from measured diffuse reflection and transmission, the wavelength-dependent anisotropy coefficient of Mie theory (Fig. 5B) was assumed. Mie theory calculations assumed a constant polystyrene index of refraction of 1.56 and constant PBS index of refraction of 1.33. Figure 5 illustrates that the size of the microspheres is a critical parameter in the selection of a scatterer to simulate the wavelength dependence of tissue scattering. The scattering coefficient and anisotropy coefficient of 5.32-μm-diameter spheres rapidly oscillate over the wavelength range from 250 to 700 nm. This phenomenon is not observed for 1.05-μm-diameter spheres; here μ_s and g closely resemble those of turbid tissues. This behavior is consistent with Mie theory predictions.[19] Figure 5A shows the value of μ_s predicted by Mie Theory for 1.05-μm-diameter spheres; the measured scattering coefficient is within 20% of the Mie theory prediction. It is important to note that, although the scattering coefficient scales linearly with concentration, the anisotropy coefficient is independent of concentration.[19] Having established that μ_s and g of 1.05-μm polystyrene spheres are appropriate for use in a tissue phantom, we must investigate the final requirement of our ideal scatterer, zero absorption. Figure 5C illustrates the absorption and scattering coefficient of a 0.625% -by-volume solution of 1.05-μm-diameter polystyrene spheres. Although the absorption coefficient of the 1.05-μm-diameter spheres at this concentration is small in comparison to the scattering coefficient (Fig. 5C) and the absorption coefficient of the 2% oxyhemoglobin absorber (Fig. 3), it is comparable to the absorption coefficient of the dilute fluorophore solutions (Fig. 1). Thus, 1.05-μm-diameter polystyrene spheres measured at a concentration of 0.625% by volume were selected for use in the phantom, since they most closely met the ideal phantom requirements.

Inhomogeneous Samples. In order to model the fluorescence of inhomogeneous, multilayer tissues, a substrate with minimal absorption, scattering, and fluorescence was sought for construction of solid phantoms. Gelatin satisfies these criteria and was selected for use as the medium from which layered samples were constructed. Fluorophores were mixed with 4 g Knox unflavored gelatin and PBS, placed into molds, and allowed to cure. Samples were subsequently cut from these molds, and layers were stacked, with thin layers of plastic wrap separating each layer to prevent chromophore diffusion. Sample thickness was measured with micrometer calipers. The gelatin index of refraction was measured to be 1.38 at 488 nm. All samples were between 1 and 2 mm thick. These were placed against one wall of a 1-cm cuvette. However, samples can also be examined in air to achieve different boundary conditions. Fluorescence and absorption spectra were collected from inhomogeneous samples in a manner identical to that used for the solutions.

Phantom Studies. Spectroscopic data were collected for each of the samples listed in Table II. In order to derive an initial understanding of the effect of scattering and absorption on fluorescence independently and in combination, the following methodology was employed:

TABLE II. Samples used in phantom studies.

Solution No.	FAD	Rhodamine B	Polystyrene	Hemoglobin	Solvent/substrate
1	20 μM	···	···	···	PBS
2	···	0.43 μM	···	···	PBS
3	20 μM	0.43 μM	···	···	PBS
4	···	···	···	2%	PBS
5	20 μM	0.43 μM	···	2%	PBS
6	···	···	0.625%	···	PBS
7	20 μM	0.43 μM	0.625%	···	PBS
8	20 μM	0.43 μM	0.625%	2%	PBS
9	3 mM	···	···	···	Gelatin
10	···	4 μM	···	···	Gelatin
11	3 mM	4 μM	···	···	Gelatin

Using an excitation wavelength of 340 nm, we acquired emission spectra for the dilute mixture containing only FAD and Rhodamine B (sample 3). A solution with the same fluorophores and polystyrene microspheres was prepared (sample 7) and the fluorescence, reflectance, and transmission spectra were recorded. To investigate the effect of an added absorber on the fluorescence of a nonscattering sample, we prepared FAD, Rhodamine B, and hemoglobin (sample 5) and acquired the spectra. Finally, to examine effects of scattering and absorption in combination, we acquired diffuse reflectance, transmission, and fluorescence emission spectra for a solution of the fluorophores, hemoglobin and polystyrene spheres (sample 8).

To investigate the effects of inhomogeneities on fluorescence spectra, we performed the following experiments: Fluorescence emission spectra were separately acquired at 488-nm excitation of two gelatin substrates, one containing FAD (sample 9) and the other containing Rhodamine B (sample 10). The layers were then stacked, and a fluorescence emission spectrum was obtained of the two layer sample (sample 11) with excitation light incident on the Rhodamine B layer.

RESULTS

Results are first presented to demonstrate how accurately absorption and scattering coefficients of fluorescent phantoms can be determined from measurements of diffuse reflection and transmission. Second, phantom fluorescence spectra are presented to demonstrate the effects of absorption, scattering, combined absorption and scattering, and sample inhomogeneities on fluorescence.

Optical Properties. Figure 6A compares the absorption coefficient determined from collimated transmission measurements for the dilute mixture containing 20 μM FAD and 0.43 μM Rhodamine B (sample 3) to that determined via inverse diffusion theory for the scattering mixture containing the same fluorophores and 0.625% polystyrene spheres (sample 7). The absorption coefficient of 0.625% polystyrene spheres (sample 6) in PBS has been subtracted from that of the 20 μM FAD, 0.43 μM Rhodamine B, 0.625% polystyrene spheres solution (sample 7). This comparison confirms that inverse diffusion theory with the delta-Eddington phase function is an appropriate method to calculate optical properties for this phantom.

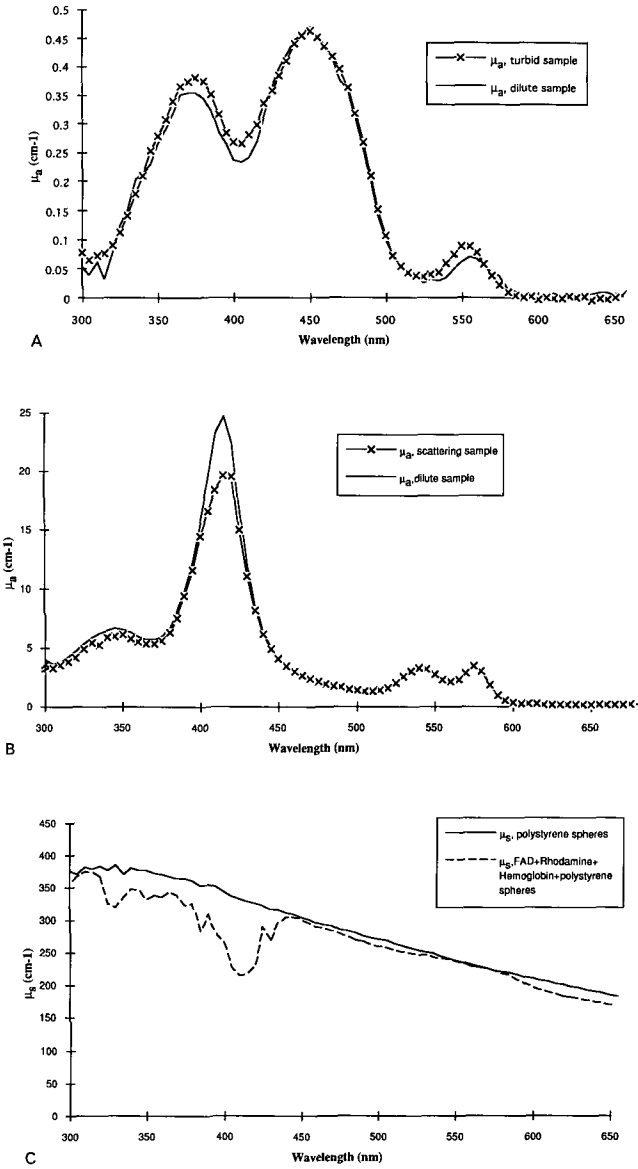

FIG. 6. (A) Absorption coefficient of dilute 20 μM FAD and 0.43 μM Rhodamine B (sample 3) determined from collimated transmission measurements vs. absorption coefficient determined via indirect methods for 20 μM FAD and 0.43 μM Rhodamine B and 0.625% polystyrene (sample 7). (B) Absorption coefficient for 20 μM FAD and 0.43 μM Rhodamine B and hemoglobin (sample 5) from collimated transmission measurements vs. absorption coefficient for 20 μM FAD and 0.43 μM Rhodamine B and hemoglobin and 0.625% polystyrene spheres (sample 8) determined via indirect methods. (C) Scattering coefficient for 0.625% polystyrene spheres vs. scattering coefficient for 20 μM FAD and 0.43 μM Rhodamine B and hemoglobin and 0.625% polystyrene spheres (sample 8). Both were determined via indirect methods.

Similarly, the absorption coefficient determined via collimated transmission measurements for the dilute mixture containing 20 μM FAD, 0.43 μM Rhodamine B, and hemoglobin (sample 5) was compared to that determined via inverse diffusion theory for 0.43 μM Rhodamine B, hemoglobin, and 0.625% polystyrene spheres (sample 8). Figure 6B illustrates that the absorption coefficient obtained for the scattering sample is in excellent agreement with that obtained for the nonscattering sample at the 543-nm and the 578-nm absorption bands of hemoglobin. There is, however, a 20% discrepancy be-

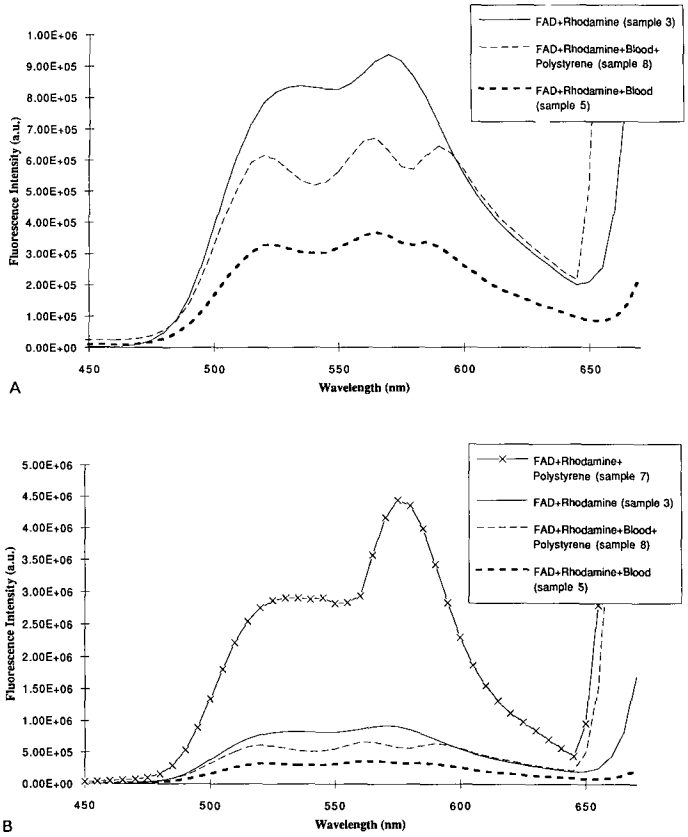

FIG. 7. (A) Fluorescence emission spectra acquired at 340-nm excitation for dilute 20 μM FAD and 0.435 μM Rhodamine B (sample 3), 20 μM FAD and 0.43 μM Rhodamine B and hemoglobin (sample 5), and 20 μM FAD and 0.43 μM Rhodamine B and hemoglobin and 0.625% polystyrene spheres (sample 8). (B) Fluorescence emission spectra acquired at 340-nm excitation of solutions containing 20 μM FAD, 0.43 μM Rhodamine B, and 0.625% polystyrene spheres (sample 7). Also shown here are the emission spectra for dilute 20 μM FAD and 0.435 μM Rhodamine B (sample 3), 20 μM FAD and 0.43 μM Rhodamine B and hemoglobin (sample 5), and 20 μM FAD and 0.43 μM Rhodamine B and hemoglobin and 0.625% polystyrene spheres (sample 8).

tween the absorption coefficients at 420 nm, with the absorption coefficient of the scattering solution being underestimated in the scattering sample. Figure 6C shows that a similar discrepancy in the scattering coefficient also exists at 420 nm. Two factors contribute to this phenomenon. First, this disparity suggests a breakdown in the ability of inverse diffusion theory to accurately predict the absorption coefficient. The sample is no longer scattering dominant [$\mu_s(1 - g) > \mu_a$; $\mu_s(1 - g) = 20$ cm^{-1}, $\mu_a = 25$ cm^{-1}] in the region of the Soret band at this particular concentration of hemoglobin.[18] Second, the ability of any model to accurately predict the optical properties is suspect in this regime because the values obtained for the transmission in the scattering sample were on the order of 1% in this region.[27]

Fluorescence Properties. Having established that the optical properties of the phantom can be accurately determined, we can now use the phantom to demonstrate the effects of absorption and scattering on fluorescence spectra when $\mu_s(1 - g) > \mu_a$. Figure 7 qualitatively illustrates the effects that result from the addition of combinations of absorber and scatterer to a dilute fluorescent solution. These fluorescence emission spectra were collected at an excitation wavelength of 340 nm. Figure 7A illustrates that the addition of hemoglobin to the nonscattering fluorescent mixture results in an overall decrease in fluorescence intensity with the greatest reduction at the 543- and 578-nm oxyhemoglobin absorption bands. The absorption band at the 578-nm band produces a valley in the fluorescence spectrum, creating an apparent third emission peak. The inclusion of a scatter in the fluorescent solution results in a dramatic increase in the measured fluorescence intensity, as depicted in Fig 7B. When hemoglobin is added to the fluorescent mixture containing polystyrene spheres, the effects of absorption are greatly enhanced in comparison to that of the nonscattering solution containing hemoglobin. Figure 7 is a qualitative illustration of the degree to which scattering and absorption can obscure the intensity and fluorescence line shape of intrinsic fluorophores contained in homogeneous samples.

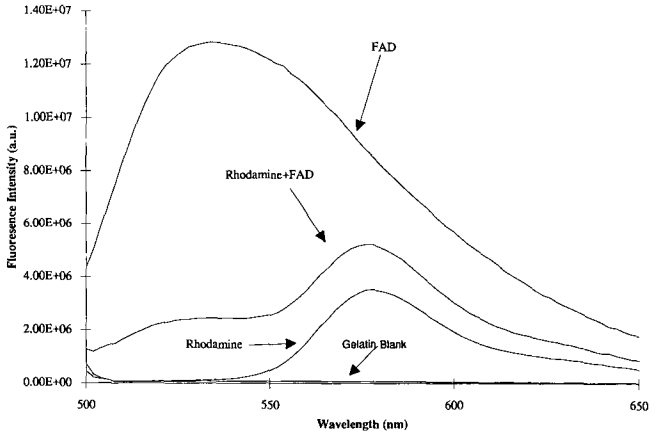

FIG. 8. Fluorescence emission spectra of gelatin based phantoms acquired at 488-nm excitation. Spectra of single layers with 3 mM FAD (sample 9) and 4 μM Rhodamine B (sample 10) and a gelatin blank are shown. Also shown is the spectrum of a two-layer phantom, the first layer containing 4 μM Rhodamine B and the second layer containing 3 mM FAD (sample 11).

Inhomogeneous Samples. Many tissues contain inhomogeneous distributions of chromophores. The phantom materials presented here can be imbedded in a gelatin matrix to simulate the effects of these inhomogeneities on fluorescence spectra. Figure 8 shows a qualitative example of the effects of layered sample structure on fluorescence. Here, fluorescence emission of two homogeneous samples [one containing FAD (sample 9), the other containing Rhodamine B (sample 10)] are compared to the fluorescence emission spectrum of the two-layer phantom constructed from these two samples (sample 11). The spectrum of the two-layer sample clearly contains contributions from both fluorophores. The relative contribution of the second layer, containing FAD, is decreased in the two-layer sample. This observation is the result of two factors: the attenuation of excitation and emission light in the first layer, and the reduced collection efficiency of the spectrometer as the layers become more distant from the in-focus spot at the sample front surface. Polystyrene microspheres can be embedded within this gelatin, providing the capability to investigate the effects of inhomogeneities on the fluorescence of turbid samples.

CONCLUSIONS

This work demonstrates that it is possible to construct a fluorescent phantom in which the optical and fluorescence properties can be controlled and accurately determined within an experimental framework that is not uncommon or exotic. These phantoms possess fundamental similarities to the optical characteristics of human tissue. We have demonstrated that one-dimensional diffusion theory can be used to accurately calculate the optical properties of phantoms containing dilute concentrations of fluorophores in the presence of scatterer and absorber as long as the $\mu_s(1 - g) > \mu_a$ assumption is satisfied. This requirement, although restrictive, is satisfied in many tissue types.[14] We have also shown that, because of the regularity in the size and shape of the coefficients, Mie theory can be used to predict the scattering coefficient and anisotropy coefficient of polystyrene microspheres within the phantom. Finally, we have qualitatively demonstrated the effects of the presence of absorber, scatterer, combination of absorber and scatterer, and sample inhomogeneities on the fluorescence spectrum of a sample containing dilute concentrations of fluorophores. Although data are presented here at 340-nm excitation, the phantom can be used over the wavelength range 300 to 650 nm and thus can be used to study fluorescence excitation emission matrices (EEMs).

The phantom provides the framework to extend these studies to the quantitative level to verify theories of fluorescence and reflection applicable to tissue systems. In addition, the phantom can be used to quantitatively study the effect of varying boundary conditions, sample size and shape, and collection geometry on fluorescence spectra. Finally, the phantom can be used to test systems for acquiring fluorescence images of scattering tissues and determine the ultimate spatial resolution which can be achieved in a turbid, inhomogeneous sample.

1. R. R. Richards-Kortum, R. Rava, M. Fitzmaurice, L. Tong, N. B. Ratliff, J. R. Kramer, and M. S. Feld, IEEE Trans. Biomed. Eng. **36,** 1222 (1989).
2. L. I. Laifer, K. M. O'Brien, M. L. Stetz, G. R. Gindi, T. J. Garrand, and L. I. Deckelbaum, Circulation **80,** No. 6, 1893 (1990).
3. R. M. Cothren, R. R. Richards-Kortum, M. V. Sivak, M. Fitzmaurice, R. P. Rava, G. A. Boyce, G. B. Hayes, M. Doxtader, R. Blackman, T. Ivanc, M. S. Feld, and R. E. Petras, Gastrointestinal Endosc. **36,** 105 (1990).
4. R. R. Alfano, A. Prahdan, and G. C. Tang, J. Opt. Soc. Amer. 1015 (1989).
5. J. R. Lakowicz, *Principles of Fluorescence Spectroscopy* (Plenum Press, New York, 1983), p. 40.
6. E. Malinowski, *Factor Analysis in Chemistry* (John Wiley & Sons, Inc, New York, 1991), p. 137.
7. M. J. C. van Gemert, A. J. Welch, W. M. Star, M. Motamedi, and W. Cheong, Lasers Med. Sci. **2,** 295 (1987).
8. J. Wu, M. S. Feld, and R. P. Rava, "An Analytical Model for Extracting Intrinsic Fluorescence in a Turbid Media," Appl. Opt. (1992), paper in press.
9. A. J. Durkin, S. Jaikumar, N. Ramanujan, and R. Richards-Kortum, "Relation Between Fluorescence Spectra of Dilute and Turbid Samples," paper submitted to Appl. Opt. (1992).
10. M. Keijzer, R. Richards-Kortum, S. L. Jacques, and M. S. Feld, Appl. Opt. **28,** 4826 (1989).
11. R. J. Crilly, W. F. Cheong, M. Motamedi, and J. R. Spears, Lasers Surg. Med. **S4,** 4 (1992).
12. C. Gardner, S. L. Jacques, and A. J. Welch, "Determination of Intrinsic Fluorescence," in *Proceedings: SPIE Biomedical Optics* (SPIE, Bellingham, Washington, 1993), in press.
13. R. Richards-Kortum, J. Zeng, A. J. Durkin, and G. Criswell, "Confocal Fluorescence Spectroscopy," invited talk, Engineering Foundation Conference, Palm Coast, Florida (1993).
14. W. F. Cheong, S. Prahl, and A. J. Welch, IEEE JQE **26,** 2166 (1990).
15. M. S. Patterson and B. C. Wilson, Appl. Opt. **28,** 2331 (1989).
16. S. Prahl, Doctoral Dissertation, The University of Texas at Austin (1988), p. 105.
17. A. J. Durkin, S. Jaikumar, and R. Richards-Kortum, "Remote Monitoring of Fluorescent Molecules in Turbid Media," in *Conference on Lasers and Electro-Optics 1992,* Vol. 12, OSA Technical Digest Genes (Optical Society of America, Washington, D.C., 1992), pp. 398–399.
18. G. Yoon, S. A. Prahl, and A. J. Welch, Appl. Opt. **28,** 2250 (1989).
19. C. F. Bohren and D. R. Huffman, *Absorption and Scattering of Light by Small Particles* (John Wiley and Sons, New York, 1983), p. 256.
20. D. G. Taylor and J. N. Demas, Anal. Chem. **51,** 712 (1979).
21. K. Yagi and T. Yamano, *Flavins and Flavoproteins* (University Park Press, Baltimore, Maryland, 1969).
22. I. D. Campbell and R. A. Dwek, *Biological Spectroscopy* (Benjamin Cummings Publishing Company, Menlo Park, California, 1984).
23. G. E. Glock and P. McClean, Cancer Res. **65,** 413 (1957).
24. *Biochemicals: Organic Compounds for Research and Diagnostic Reagents* (Sigma Chemical Company, St. Louis, Missouri, 1992), p. 688.
25. C. J. M. Moes, M. J. C. van Gemert, W. M. Star, J. P. A. Marijnissen, and S. A. Prahl, Appl. Opt. **28,** 2292 (1989).
26. F. W. J. Teale, Photochem. Photobiol. **10,** 363 (1969).
27. S. A. Prahl, M. C. J. van Gemert, and A. J. Welch, Appl. Opt. **32,** 559 (1993).